results from two chelating phen moieties and three bidentate NO_3^- ions. These results are in excellent agreement with data previously reported for the corresponding complexes of heavier Ln(III) ions which were isolated in the solid state.[11,34] Concerning the two other species, La^{III} and La^{III}(phen), the chemical formulas should include undetermined amounts of H_2O and CH_3CN, in addition to the three NO_3^- ions and the phen molecule (1:1 complex). Accordingly, one should formulate them as $[La(NO_3)_3(H_2O)_x(CH_3CN)_y]$ and $[La(NO_3)_3(phen)(H_2O)_w(CH_3CN)_z]$, respectively.

By addition of hydrated lanthanum(III) nitrate and phen in CH_3CN, a competition is established between phen, NO_3^-, H_2O, and CH_3CN for the occupancy of the coordination sites on La(III). During the course of the complexation of La(III) by phen, the three coordinated NO_3^- groups remain bound to La(III) whereas water and CH_3CN are substituted. No NMR spectral evidence of competition between phen and NO_3^- was noted, indicating that NO_3^- is a much stronger stabilizing species than phen. The ^{17}O NMR results show that some water is coordinated to La(III) in both La^{III} and La^{III}(phen) even though its total concentration in solution is much lower than that of the solvent CH_3CN. From these results, it comes that the decreasing coordinating strength for La(III) is $NO_3^- >$ phen $> H_2O > CH_3CN$.

An analysis of log K_i for the successive coordination of phen to La(III) (see Table IV) shows a decrease when going from log K_1 to log K_2. This decrease is in good agreement with other studies and results from statistical factors.[35] On the basis of this statistical factor only, log K_3 should not be higher than 1.0. This estimation is valid only if the ligands expelled are the same throughout the complexation steps. Since the addition of a third phen ligand could be done only at the expense of a much stronger ligand than CH_3CN or H_2O, namely NO_3^-, the resulting log K_3 value should be much smaller than 1.0.

Since water is also substituted during the course of the complexation, the actual equilibrium processes involved in the complexation of La(III) with phen are not as simple as it appears above. To write a complete thermodynamic scheme of the complexation processes in solution would necessitate the exact knowledge of the water content in the coordination sphere of La^{III} and of La^{III}(phen). From the ^{17}O NMR data, one knows that very small amounts of water are coordinated to the inner sphere of La^{III} and La^{III}(phen). For this first study of the system, this validates the simplification of considering only the displacement of CH_3CN in the equations describing the complexation process. A more complete thermodynamic treatment based on ^{17}O and ^{139}La NMR data as well as on potentiometric methods will be published later.[29]

Acknowledgment. The Natural Sciences and Engineering Research Council of Canada (NSERCC) is gratefully acknowledged for an Operating Grant to C.D. "Le Conseil de l'Education Franco-Ontarienne" (CEFO) is acknowledged for a Professorship and an Operating Grant to M.F. A grant for the purchase of a Karl-Fisher titrimeter, from the Development Fund of the Faculty of Science of the University of Ottawa, is also acknowledged. We thank Dr. Corinne Bensimon, University of Ottawa, for valuable discussions.

Registry No. $La(NO_3)_3(phen)_2$, 139758-78-4.

Supplementary Material Available: Table S-I–S-V, listing respectively crystallographic data, calculated hydrogen atom parameters, anisotropic temperature factors, bond distances, and bond angles (4 pages); Table S-VI, listing structure factors (13 pages). Ordering information is given on any current masthead page.

---

(34) Lobanov, N. I.; Smirnova, V. A. *Russ. J. Inorg. Chem.* (*Engl. Transl.*) **1963**, *8*, 1154.

(35) Cotton, F. A.; Wilkinson, G. *Advanced Inorganic Chemistry*; 5thd ed.; John Wiley & Sons: Toronto, Canada, 1988; pp 41–45.

Contribution from the Department of Chemistry,
Columbia University, New York, New York 10027

Resolved and Unresolved Crystallographic Disorder between $\{\eta^3\text{-HB(3-Bu}^t\text{pz)}_3\}\text{ZnCN}$ and $\{\eta^3\text{-HB(3-Bu}^t\text{pz)}_3\}\text{ZnX}$ (X = Cl, Br, I)

Keum Yoon and Gerard Parkin*

Received October 17, 1991

Crystallographic disorder between structurally inequivalent groups has been investigated by X-ray diffraction studies. By use of a technique in which a crystal is doped with an impurity, the disorder at a single site was varied in a controlled fashion. Specifically, single crystals of composition $\{\eta^3\text{-HB(3-Bu}^t\text{pz)}_3\}\text{Zn(CN)}_x\text{X}_{1-x}$ (3-Bu^{t}pz = 3-$C_3N_2H_2Bu^t$; X = Cl, Br, I; $0 \leq x \leq 1$) were obtained by cocrystallization of $\{\eta^3\text{-HB(3-Bu}^t\text{pz)}_3\}\text{ZnCN}$ and $\{\eta^3\text{-HB(3-Bu}^t\text{pz)}_3\}\text{ZnX}$. Although disorder between (i) CN and Cl and (ii) CN and Br was not resolved, the disorder between CN and I in $\{\eta^3\text{-HB(3-Bu}^t\text{pz)}_3\}\text{Zn(CN)}_{0.9}\text{I}_{0.1}$ was readily apparent, and the individual groups could be refined with surprising success. However, the bond lengths obtained from the disordered structure were incorrect, as judged by comparison with the pure structures. Thus, although satisfactory refinement of a disordered structure may be taken as good evidence for the nature of the disorder, and therefore a good indication of the molecular structure, attempts to extract the *true* bond lengths from such a structure must be treated with caution. Crystal data are as follows. $\{\eta^3\text{-HB(3-Bu}^t\text{pz)}_3\}\text{ZnCN}$: orthorhombic, *Pnma* (No. 62), a = 16.315 (3) Å, b = 15.852 (3) Å, c = 9.757 (2) Å, V = 2523 (1) Å^3, Z = 4. $\{\eta^3\text{-HB(3-Bu}^t\text{pz)}_3\}\text{Zn(CN)}_{0.8}\text{Cl}_{0.2}$: orthorhombic, *Pnma* (No. 62), a = 16.235 (2) Å, b = 15.871 (3) Å, c = 9.760 (1) Å, V = 2514 (1) Å^3, Z = 4. $\{\eta^3\text{-HB(3-Bu}^t\text{pz)}_3\}\text{Zn(CN)}_{0.95}\text{Br}_{0.05}$: orthorhombic, *Pnma* (No. 62), a = 16.303 (4) Å, b = 15.847 (6) Å, c = 9.752 (3) Å, V = 2519 (1) Å^3, Z = 4. $\{\eta^3\text{-HB(3-Bu}^t\text{pz)}_3\}\text{Zn(CN)}_{0.9}\text{I}_{0.1}$: orthorhombic, *Pnma* (No. 62), a = 16.315 (6) Å, b = 15.841 (8) Å, c = 9.751 (4) Å, V = 2520 (1) Å^3, Z = 4.

Introduction

Our recent investigations have demonstrated that the original report of "distortional"[1] or "bond-stretch"[2] isomerism is an artifact due to crystallographic disorder.[3] The observation of "isomers" of *cis-mer*-$MoOCl_2(PMe_2Ph)_3$, with apparently different Mo═O bond lengths, is due to cocrystallization with small quantities of

---

(1) (a) Chatt, J.; Manojlovic-Muir, L.; Muir, K. W. *Chem. Commun.* **1971**, 655–656. (b) Manojlovic-Muir, L. *J. Chem. Soc. A* **1971**, 2796–2800. (c) Manojlovic-Muir, L.; Muir, K. W. *J. Chem. Soc., Dalton Trans.* **1972**, 686–690. (d) Haymore, B. L.; Goddard, W. A., III; Allison, J. N. *Proc. Int. Conf. Coord. Chem., 23rd* **1984**, 535.

(2) (a) Jean, Y.; Lledos, A.; Burdett, J. K.; Hoffmann, R. *J. Am. Chem. Soc.* **1988**, *110*, 4506–4516. (b) Jean, Y.; Lledos, A.; Burdett, J. K.; Hoffmann, R. *J. Chem. Soc., Chem. Commun.* **1988**, 140–142.

(3) (a) Yoon, K.; Parkin, G.; Rheingold, A. L. *J. Am. Chem. Soc.* **1991**, *113*, 1437–1438. (b) Yoon, K.; Parkin, G.; Rheingold, A. L. *J. Am. Chem. Soc.* **1992**, *114*, 2210–2218.

0020-1669/92/1331-1656$03.00/0

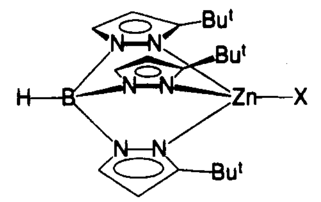

Figure 1. Molecular structure of $\{\eta^3\text{-HB(3-Bu}^t\text{pz)}_3\}$ZnX.

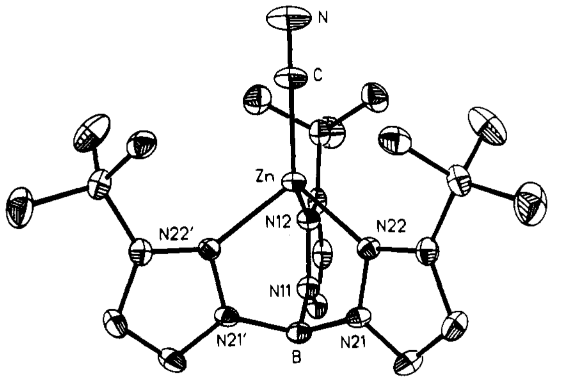

Figure 2. ORTEP drawing for $\{\eta^3\text{-HB(3-Bu}^t\text{pz)}_3\}$ZnCN (20% thermal ellipsoids).

the isostructural trichloride complex *mer*-$MoCl_3(PMe_2Ph)_3$. Partial occupancy of the oxo site by a chloride ligand leads to an *apparent* increase of the "Mo=O" bond length, since the chloride ligand is located at a much greater distance from the molybdenum center. Unfortunately, disorder of this nature may not be *readily* apparent by examination of X-ray diffraction data alone. Indeed, it is presumably because such disordered sites may refine well as an ordered site that this explanation was not considered when the suggestion of "distortional" isomerism was first proposed.[1] Experimental evidence for the concept of "bond-stretch" isomerism may represent an extreme example of an artifact due to crystallographic disorder; however, problems derived from undetected crystallographic disorder resulting in the observation of incorrect bond lengths may be much more widespread than presently realized. The recent report of significantly different bond lengths [2.437 (1) and 2.295 (2) Å] for the two *chemically equivalent* W–Cl_{trans} bonds in *mer*-$WCl_3(PMe_2Ph)_3$ is one such example.[4] It is evident from our additional studies that this inequivalence is an artifact due to cocrystallization with the *oxo* complex *cis-mer*-$WOCl_2(PMe_2Ph)_3$, which serves to *apparently* shorten one of the W–Cl bond lengths.[5] The above results highlight the fact that the presence of an impurity in a single-crystal may have a profound consequence upon an X-ray structure determination. We have recently investigated controlled crystallographic disorder in a series of solid solutions of pairs of the structurally related [tris(3-*tert*-butylpyrazolyl)hydroborato]zinc complexes, $\{\eta^3\text{-HB(3-Bu}^t\text{pz)}_3\}$ZnX (3-$Bu^t$pz = 3-$C_3N_2H_2Bu^t$; X = Cl, Br, I, CH_3), shown in Figure 1,[6] and here we describe further studies in order to examine controlled disorder between groups that are *not* isostructural.

Results

The molecular structure of the cyanide complex $\{\eta^3\text{-HB(3-Bu}^t\text{pz)}_3\}$ZnCN has been determined by X-ray diffraction. ORTEP drawings for $\{\eta^3\text{-HB(3-Bu}^t\text{pz)}_3\}$ZnCN are given in Figures 2 and 3, while atomic coordinates and selected bond lengths and angles are listed in Tables I and II. $\{\eta^3\text{-HB(3-Bu}^t\text{pz)}_3\}$ZnCN is isomorphous with the previously reported complexes $\{\eta^3\text{-HB(3-Bu}^t\text{pz)}_3\}$ZnX (X = Cl, Br, I),[6] and solutions of mixtures of $\{\eta^3\text{-HB(3-Bu}^t\text{pz)}_3\}$ZnCN and $\{\eta^3\text{-HB(3-Bu}^t\text{pz)}_3\}$ZnX (X = Cl, Br, I) give single crystals composed of a solid solution of the respective complexes. These single-crystal solid solutions have been investigated by X-ray diffraction methods, the results of which are described below.

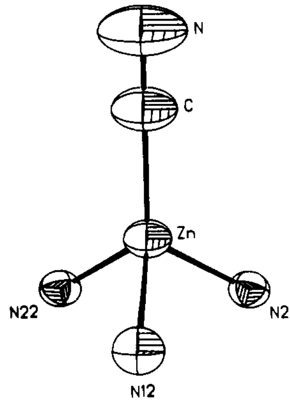

Figure 3. Partial ORTEP drawing for $\{\eta^3\text{-HB(3-Bu}^t\text{pz)}_3\}$ZnCN (50% thermal ellipsoids).

Table I. Atom Coordinates (×10^4) and Temperature Factors (Å^2 × 10^3) for $\{\eta^3\text{-HB(3-Bu}^t\text{pz)}_3\}$ZnCN

atom	*x*	*y*	*z*	*U*[a]
Zn	1620 (1)	7500	5950 (1)	41 (1)
C	464 (4)	7500	5395 (7)	60 (3)
N	−194 (4)	7500	5078 (7)	98 (3)
N(11)	3288 (3)	7500	5146 (5)	46 (2)
N(12)	2529 (3)	7500	4512 (5)	44 (2)
N(21)	2955 (2)	8290 (2)	7300 (3)	43 (1)
N(22)	2135 (2)	8443 (2)	7094 (3)	41 (1)
C(11)	3875 (4)	7500	4186 (7)	51 (2)
C(12)	3509 (4)	7500	2928 (7)	60 (3)
C(13)	2665 (4)	7500	3160 (6)	46 (2)
C(14)	1973 (4)	7500	2126 (7)	58 (3)
C(15)	2333 (5)	7500	688 (6)	95 (4)
C(16)	1443 (3)	8287 (3)	2326 (5)	85 (2)
C(21)	3267 (3)	8894 (3)	8090 (5)	59 (2)
C(22)	2665 (3)	9450 (3)	8426 (5)	60 (2)
C(23)	1954 (3)	9150 (3)	7794 (4)	47 (2)
C(24)	1100 (3)	9518 (3)	7843 (5)	53 (2)
C(25)	1094 (3)	10267 (3)	8827 (6)	98 (3)
C(26)	495 (2)	8872 (3)	8397 (5)	60 (2)
C(27)	842 (3)	9809 (4)	6427 (5)	99 (3)
B	3373 (5)	7500	6719 (7)	46 (3)

[a] Equivalent isotropic *U* defined as one-third of the trace of the orthogonalized U_{ij} tensor.

Discussion

Crystallographic disorder, in which a site is partially occupied by different atoms (or groups), is well-known. However, the presence of a disorder is normally only discerned at the stage of refinement when an anomaly, e.g. unusual thermal parameters or residual electron density, is detected. Indeed, such examples normally represent crystallographic problem structures and have been solved with different degrees of success. Crystallographic disorder in single crystals has not previously been studied in a systematic fashion, and our recent studies have shown that disorder may exert very subtle effects upon a crystal structure determination. In particular, changes in apparent bond lengths may be much more sensitive to the disorder than either electron density distributions or thermal parameters. Thus, crystallographic disorder may often go undetected, even though apparent bond lengths may be influenced. It is for such examples that it is important to appreciate the effects that disorder may have upon an observed structure. In view of the sensitivity of apparent bond lengths to disorder, it is important to investigate the structures of well-defined systems in which the disorder may be controlled. The most common source of disorder is derived from packing equivalent molecules in different orientations; however, it is difficult (if not impossible) to control such disorder in a defined manner. A simpler method for controlling disorder at a crys-

---

(4) Hills, A.; Hughes, D. L.; Leigh, G. J.; Prieto-Alcón, R. *J. Chem. Soc., Dalton Trans.* **1991**, 1515–1517.

(5) Yoon, K.; Parkin, G.; Hills, A.; Hughes, D. L.; Leigh, G. J.; Prieto-Alcón, R. *J. Chem. Soc., Dalton Trans.*, in press.

(6) Yoon, K.; Parkin, G. *J. Am. Chem. Soc.* **1991**, *113*, 8414–8418.

Table II. Selected Bond Lengths (Å) and Angles (deg) for $\{\eta^3$-HB(3-Bu^{t}pz)$_3\}$Zn(CN)$_x$X$_{1-x}$ (X = Cl, Br, I)

	LZnCN	LZn(CN)$_{0.8}$Cl$_{0.2}$	LZn(CN)$_{0.95}$Br$_{0.05}$	LZn(CN)$_{0.9}$I$_{0.1}$	LZnI[a]
Zn–C[b]	1.962 (6)	2.094 (4)	2.035 (6)	1.932 (12)	
Zn–X[c]				2.469 (8)	2.518 (1)
C–N	1.117 (9)	0.996 (9)	1.058 (9)	1.178 (15)	
C–X[c]				0.549 (15)	
Zn–N(12)	2.041 (5)	2.037 (4)	2.039 (4)	2.035 (4)	2.073 (5)
Zn–N(22)	2.047 (3)	2.046 (2)	2.045 (3)	2.050 (3)	2.068 (3)
Zn–C–N	180.0 (6)	177.6 (5)	179.3 (6)	178.6 (13)	
C(X)–Zn–N(12)	120.6 (2)	121.1 (1)	120.9 (2)	121.3 (5)	120.3 (1)
C(X)–Zn–N(22)	123.0 (1)	122.7 (1)	122.9 (1)	122.7 (2)	123.1 (1)
N(12)–Zn–N(22)	94.4 (1)	94.5 (1)	94.4 (1)	94.5 (1)	95.2 (1)
N(22)–Zn–N(22′)	93.8 (2)	93.8 (1)	93.8 (2)	93.6 (2)	92.6 (2)

[a] Taken from ref 6. [b] For the disordered structures the distance reported is the *apparent* bond length. [c] Only listed for resolved structures.

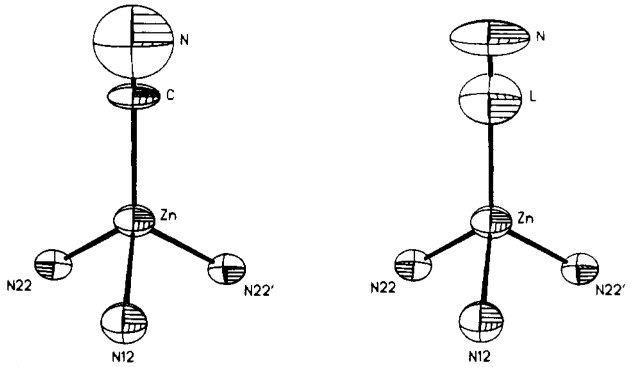

Figure 4. Partial ORTEP drawings for $\{\eta^3$-HB(3-Bu^{t}pz)$_3\}$Zn(CN)$_{0.8}$Cl$_{0.2}$ (50% thermal ellipsoids). Left: disordered site refined as CN only. Right: disordered site refined as (CN)$_{0.76(1)}$Cl$_{0.24(1)}$, where L = C$_{0.76(1)}$Cl$_{0.24(1)}$ and N = N$_{0.76(1)}$.

Table III. Atom Coordinates (×10^4) and Temperature Factors (Å^2 × 10^3) for $\{\eta^3$-HB(3-Bu^{t}pz)$_3\}$Zn(CN)$_{0.8}$Cl$_{0.2}$

atom	*x*	*y*	*z*	*U*[a]
Zn	1622 (1)	7500	5955 (1)	38 (1)
C	380 (3)	7500	5381 (4)	77 (2)
Cl	380 (3)	7500	5381 (4)	77 (2)
N	−204 (4)	7500	5066 (7)	91 (3)
N(11)	3293 (2)	7500	5143 (4)	42 (1)
N(12)	2534 (2)	7500	4521 (4)	42 (1)
N(21)	2960 (1)	8288 (2)	7297 (3)	41 (1)
N(22)	2137 (1)	8441 (2)	7103 (2)	38 (1)
C(11)	3882 (3)	7500	4185 (5)	50 (2)
C(12)	3516 (3)	7500	2921 (6)	57 (2)
C(13)	2670 (3)	7500	3162 (5)	48 (2)
C(14)	1971 (4)	7500	2127 (5)	61 (2)
C(15)	2331 (4)	7500	681 (5)	93 (3)
C(16)	1443 (3)	8295 (3)	2334 (4)	78 (2)
C(21)	3277 (2)	8888 (2)	8093 (4)	53 (1)
C(22)	2673 (2)	9450 (2)	8431 (4)	56 (1)
C(23)	1960 (2)	9152 (2)	7790 (3)	42 (1)
C(24)	1104 (2)	9522 (2)	7858 (4)	51 (1)
C(25)	1104 (3)	10274 (3)	8830 (5)	91 (2)
C(26)	499 (2)	8869 (2)	8407 (4)	57 (1)
C(27)	835 (3)	9798 (3)	6432 (5)	92 (2)
B	3382 (3)	7500	6709 (5)	42 (2)

[a] Equivalent isotropic *U* defined as one-third of the trace of the orthogonalized U$_{ij}$ tensor.

tallographic site involves doping a crystal with structurally similar molecules. Importantly, this method allows the composition of the disordered site to be determined by a method that is independent of the disorder model used for refinement. Here we describe the use of this method in order to investigate systematically the consequences of disorder between groups that are *not* isostructural, in a system composed of $\{\eta^3$-HB(3-Bu^{t}pz)$_3\}$ZnX complexes.

Disorder between groups that are not isostructural is well-known, with many instances involving disorder between carbonyl and other ligands, e.g. *trans*-IrCl(CO)(PPh$_3$)$_2$,[7] *trans*-RhCl(CO)(PPh$_3$)$_2$,[8,9] *trans*-IrCl(CO)[P(C$_6$H$_4$-*o*-CH$_3$)$_3$]$_2$,[10] *trans*-Ir(CH$_3$)(CO)(PPh$_3$)$_2$,[11] *trans*-Ir(OCH$_3$)(CO)(PPh$_3$)$_2$,[12] IrI(CO)(O$_2$)(PPh$_3$)$_2$,[13] and IrCl(CO)(O$_2$)(PPh$_3$)$_2$.[14] Other examples of disorder between structurally inequivalent groups have been observed between N$_2$ and Cl in the complexes [W(PMe$_3$)$_4$(N$_2$)$_2$]/[W(PMe$_3$)$_4$Cl$_2$],[15] [*trans*-Cr(dmpe)$_2$(N$_2$)$_2$]/[*trans*-Cr(dmpe)$_2$Cl$_2$] (dmpe = Me$_2$PCH$_2$CH$_2$PMe$_2$),[16] and *trans*-ReCl(N$_2$)(PMe$_2$Ph)$_4$.[17] Furthermore, disorder between methyl (CH$_3$) and ethylidyne (C≡CH$_3$) ligands in the complex W(PMe$_3$)$_4$(CH$_3$)(CCH$_3$) resulted in the molecule originally being formulated as the dimethyl derivative W(PMe$_3$)$_4$(CH$_3$)$_2$.[18] Specifically, for the present study we chose to investigate the effect that partial occupancy by a halide ligand (X = Cl, Br, I) may have upon the apparent structure of the cyanide derivative $\{\eta^3$-HB(3-Bu^{t}pz)$_3\}$ZnCN. By varying the halide ligand from chloride to iodide, the location of the disordered atom with respect to the C≡N group may be varied. Single crystals of $\{\eta^3$-HB(3-Bu^{t}pz)$_3\}$ZnCN doped with $\{\eta^3$-HB(3-Bu^{t}pz)$_3\}$ZnX (X = Cl, Br, I) were readily prepared by cocrystallization from dichloromethane or THF solutions and were analyzed by X-ray diffraction. After data collection, the composition of each crystal was determined by ^{1}H NMR spectroscopy.

ORTEP drawings for a chloride-doped crystal of composition $\{\eta^3$-HB(3-Bu^{t}pz)$_3\}$Zn(CN)$_{0.8}$Cl$_{0.2}$ are shown in Figure 4. The ORTEP drawing on the left-hand side of Figure 4 represents a solution in which the disorder was neglected, i.e. one in which the crystal was considered to be pure $\{\eta^3$-HB(3-Bu^{t}pz)$_3\}$ZnCN. Comparison of the thermal ellipsoids associated with the cyanide ligand of $\{\eta^3$-HB(3-Bu^{t}pz)$_3\}$Zn(CN)$_{0.8}$Cl$_{0.2}$ (left-hand side of Figure 4) and pure $\{\eta^3$-HB(3-Bu^{t}pz)$_3\}$ZnCN (Figure 3) reveals an unsatisfactory solution. Specifically, the thermal ellipsoid of the

---

(7) Churchill, M. R.; Fettinger, J. C.; Buttrey, L. A.; Barkan, M. D.; Thompson, J. S. *J. Organomet. Chem.* **1988**, *340*, 257–266.

(8) Del Pra, A.; Zanotti, G.; Segula, P. *Cryst. Struct. Commun.* **1979**, *8*, 959–964.

(9) Rheingold, A. L.; Geib, S. J. *Acta Crystallogr.* **1987**, *C43*, 784–786.

(10) Brady, R.; De Camp, W. H.; Flynn, B. R.; Schneider, M. L.; Scott, J. D.; Vaska, L.; Werneke, M. F. *Inorg. Chem.* **1975**, *14*, 2669–2675.

(11) Rees, W. M.; Churchill, M. R.; Li, Y.-J.; Atwood, J. D. *Organometallics* **1985**, *4*, 1162–1167.

(12) Fettinger, J. C.; Churchill, M. R.; Bernard, K. A.; Atwood, J. D. *J. Organomet. Chem.* **1988**, *340*, 377–388.

(13) McGinnety, J. A.; Doedens, R. J.; Ibers, J. A. *Inorg. Chem.* **1967**, *6*, 2243–2250.

(14) La Placa, S. J.; Ibers, J. A. *J. Am. Chem. Soc.* **1965**, *87*, 2581–2586.

(15) Carmona, E.; Marin, J. M.; Poveda, M. L.; Atwood, J. L.; Rogers, R. D. *Polyhedron* **1983**, *2*, 185–193.

(16) (a) Girolami, G. S.; Salt, J. E.; Wilkinson, G.; Thornton-Pett, M.; Hursthouse, M. B. *J. Am. Chem. Soc.* **1983**, *105*, 5954–5956. (b) Salt, J. E.; Girolami, G. S.; Wilkinson, G.; Motevalli, M.; Thornton-Pett, M.; Hursthouse, M. B. *J. Chem. Soc., Dalton Trans.* **1985**, 685–692.

(17) Davis, B. R.; Ibers, J. A. *Inorg. Chem.* **1971**, *10*, 578–585.

(18) (a) Jones, R. A.; Wilkinson, G.; Galas, A. M. R.; Hursthouse, M. B. *J. Chem. Soc., Chem. Commun.* **1979**, 926–927. (b) Chiu, K. W.; Jones, R. A.; Wilkinson, G.; Galas, A. M. R.; Hursthouse, M. B.; Malik, K. M. A. *J. Chem. Soc., Dalton Trans.* **1981**, 1204–1211.

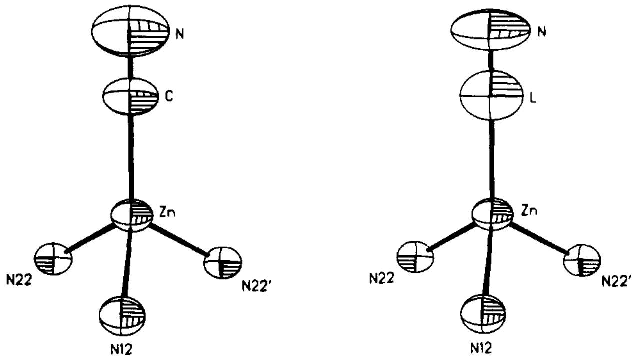

Figure 5. Partial ORTEP drawings for $\{\eta^3\text{-HB(3-Bu}^t\text{pz)}_3\}\text{Zn(CN)}_{0.95}\text{Br}_{0.05}$ (50% thermal ellipsoids). Left: disordered site refined as CN only. Right: disordered site refined as $(\text{CN})_{0.96(1)}\text{Br}_{0.04(1)}$, where L = $\text{C}_{0.96(1)}\text{Br}_{0.04(1)}$ and N = $\text{N}_{0.96(1)}$.

nitrogen atom is greatly enlarged compared with that for the pure complex, whereas the thermal ellipsoid of the carbon atom is reduced. Such behavior is anticipated: the chloride dopant would be located much closer to carbon than the nitrogen of the cyanide ligand, thus resulting in an increase in electron density at the carbon site and a reduction of electron density at the nitrogen site, which is now only partially occupied.

As we have observed previously for disorder between chloride and methyl groups in solid solutions of $\{\eta^3\text{-HB(3-Bu}^t\text{pz)}_3\}\text{Zn(CH}_3)_x\text{Cl}_{1-x}$,[6] the disorder between the chloride and the carbon of the cyanide ligand was not resolved. Here we are using the term "resolve" to indicate whether separate "peaks" are observed in an electron density difference map after locating all non-hydrogen atoms other than those at the disordered site.[19] We do not intend to imply that it is not possible to resolve atoms at disordered sites in examples where separate peaks are not observed in an electron density difference map; however, resolution of this type requires knowledge that a particular site may be disordered so that an appropriate model may be implemented.

The disordered site in $\{\eta^3\text{-HB(3-Bu}^t\text{pz)}_3\}\text{Zn(CN)}_x\text{Cl}_{1-x}$ was modeled by refining the carbon site as a composite of chlorine and carbon. The occupancies of chlorine and carbon were refined subject to the constraints that their sum was unity and also that the site occupancy of the carbon equaled that of nitrogen. The results of this refinement procedure are illustrated on the right-hand side of Figure 4. The composition of the crystal as determined by refining cyanide and chloride site occupancies is $\{\eta^3\text{-HB(3-Bu}^t\text{pz)}_3\}\text{Zn(CN)}_{0.76(1)}\text{Cl}_{0.24(1)}$, in close agreement with $\{\eta^3\text{-HB(3-Bu}^t\text{pz)}_3\}\text{Zn(CN)}_{0.8}\text{Cl}_{0.2}$ as determined by ^{1}H NMR spectroscopy. Atomic coordinates and selected bond lengths and angles for this refinement procedure are presented in Tables II and III. Significantly, the *apparent* Zn—C bond length [2.094 (4) Å] is observed to be longer than that for the pure complex [1.962 (6) Å], and the C≡N bond length [0.996 (9) Å] is correspondingly shorter than that for the pure complex [1.117 (9) Å]. The overall distance between zinc and the nitrogen of the cyanide ligand [3.09 (1) Å] is similar to that observed in pure $\{\eta^3\text{-HB(3-Bu}^t\text{pz)}_3\}\text{ZnCN}$ [3.08 (1) Å]. Thus, the role of the chloride impurity serves mainly to shift the apparent position of the carbon atom away from zinc and toward nitrogen, thereby apparently shortening the C≡N bond length. A similar explanation has been previously proposed for trans disorder between N_2 and Cl in the complex *trans*-$\text{ReCl(N}_2)(\text{PMe}_2\text{Ph})_4$,[17] for which an apparent N–N bond length of 0.94 Å, shorter than that for free N_2 [1.0976 (1) Å],[20] was originally observed. After the disorder was modeled, a substantially longer N–N bond length of 1.06 (3) Å was derived. However, a possible anomaly was not considered in the original report of an unusually short N–N bond length of 0.985 (4) Å for the complex *trans*-$\text{Cr(dmpe)}_2(\text{N}_2)_2$.[16a] Indeed, since the trans ligands are identical, there is no possibility of intramolecular disorder of the type proposed for *trans*-$\text{ReCl(N}_2)(\text{PMe}_2\text{Ph})_4$. Subsequent work has suggested that the origin of the unusually short N–N bond length in this molecule is *compositional* disorder with the *chloride impurity*, *trans*-$\text{Cr(dmpe)}_2\text{Cl}_2$.[16b] Disorder between the N atom coordinated to Cr and the Cl impurity was neither resolved nor detected, with the result that a N–N bond length shorter than that in N_2 was originally reported.[16] It is likely that other examples of undetected and unresolved disorder between monoatomic and diatomic groups may be common.[21]

Table IV. Atom Coordinates (×10^4) and Temperature Factors (Å^2 × 10^3) for $\{\eta^3\text{-HB(3-Bu}^t\text{pz)}_3\}\text{Zn(CN)}_{0.95}\text{Br}_{0.05}$

atom	*x*	*y*	*z*	U^a
Zn	1622 (1)	7500	5955 (1)	37 (1)
C	422 (4)	7500	5384 (5)	76 (3)
Br	422 (4)	7500	5384 (5)	76 (3)
N	−200 (4)	7500	5073 (7)	93 (3)
N(11)	3294 (2)	7500	5143 (4)	43 (1)
N(12)	2534 (3)	7500	4523 (4)	41 (1)
N(21)	2957 (2)	8290 (2)	7305 (3)	42 (1)
N(22)	2136 (2)	8442 (2)	7103 (3)	39 (1)
C(11)	3880 (4)	7500	4181 (6)	50 (2)
C(12)	3517 (4)	7500	2924 (6)	55 (2)
C(13)	2665 (4)	7500	3162 (5)	46 (2)
C(14)	1971 (4)	7500	2133 (6)	56 (2)
C(15)	2322 (5)	7500	689 (6)	88 (3)
C(16)	1456 (4)	8295 (3)	2331 (5)	79 (2)
C(21)	3273 (2)	8892 (3)	8104 (4)	53 (1)
C(22)	2666 (2)	9449 (3)	8438 (4)	56 (1)
C(23)	1954 (2)	9154 (2)	7793 (4)	43 (1)
C(24)	1102 (3)	9522 (3)	7857 (4)	52 (1)
C(25)	1095 (3)	10269 (3)	8842 (6)	89 (2)
C(26)	495 (2)	8863 (3)	8401 (4)	56 (1)
C(27)	841 (3)	9806 (4)	6426 (5)	93 (2)
B	3383 (3)	7500	6709 (6)	39 (2)

[a] Equivalent isotropic *U* defined as one-third of the trace of the orthogonalized U_{ij} tensor.

ORTEP drawings for a bromide-doped crystal of composition $\{\eta^3\text{-HB(3-Bu}^t\text{pz)}_3\}\text{Zn(CN)}_{0.95}\text{Br}_{0.05}$ are shown in Figure 5. The ORTEP drawing shown on the left-hand side of Figure 5 represents a solution in which the disorder was neglected, i.e. one in which the crystal was considered to be pure $\{\eta^3\text{-HB(3-Bu}^t\text{pz)}_3\}\text{ZnCN}$. Comparison of the thermal ellipsoids associated with the cyanide ligand of $\{\eta^3\text{-HB(3-Bu}^t\text{pz)}_3\}\text{Zn(CN)}_{0.95}\text{Br}_{0.05}$ (left-hand side of Figure 5) and pure $\{\eta^3\text{-HB(3-Bu}^t\text{pz)}_3\}\text{ZnCN}$ (Figure 3) reveals a solution that may be considered to be satisfactory. However, the bond lengths associated with the CN ligand are incorrect, with a long Zn—C bond length [2.018 (5) Å] and a short C≡N bond length [1.040 (8) Å]. Since the disorder with the bromide was not resolved, we chose to model the disorder by refining the carbon site as a composite of bromine and carbon, in a manner similar to that described above. The composition of the crystal as determined by refining cyanide and bromide site occupancies is $\{\eta^3\text{-HB(3-Bu}^t\text{pz)}_3\}\text{Zn(CN)}_{0.96(1)}\text{Br}_{0.04(1)}$, in close agreement with $\{\eta^3\text{-HB(3-Bu}^t\text{pz)}_3\}\text{Zn(CN)}_{0.95}\text{Br}_{0.05}$ as determined by ^{1}H NMR spectroscopy. The bond lengths associated with the CN group obtained by this procedure [*d*(Zn—C) = 2.035 (6) Å; *d*(C≡N) = 1.058 (9) Å] are slightly different from those obtained by neglecting the disorder. Atomic coordinates and selected bond lengths and angles for the latter refinement procedure are presented in Tables II and IV. Although a reasonably good solution was obtained for $\{\eta^3\text{-HB(3-Bu}^t\text{pz)}_3\}\text{Zn(CN)}_{0.95}\text{Br}_{0.05}$ by neglecting the disorder, the structure of a more bromide-rich crystal of composition $\{\eta^3\text{-HB(3-Bu}^t\text{pz)}_3\}\text{Zn(CN)}_{0.55}\text{Br}_{0.45}$ could not be solved

---

(19) The term "peaks" refers to sets of coordinates generated by the peak-searching routine of SHELXTL, not necessarily to true electron density maxima.

(20) *CRC Handbook of Chemistry and Physics*, 69th ed.; Weast, R. C., Ed.; CRC Press Inc.: Boca Raton, FL, 1988; p F-166.

(21) (a) A further example of unresolved disorder between chloride and a diatomic group has recently been suggested[21b] for *trans*-$\text{Rh(PBu}^t{}_3)_2(\text{CO})\text{Cl}$, for which a C–O bond length of 0.987 (11) Å,[21c] *shorter* than that in free CO (1.128 Å), is observed. (b) Sherwood, D. E., Jr.; Hall, M. B. *Inorg. Chem.* **1983**, *22*, 93–100. (c) Schumann, H.; Heisler, M.; Pickardt, J. *Chem. Ber.* **1977**, *110*, 1020–1026.

Table V. Atom Coordinates (×10⁴) and Temperature Factors (Å² × 10³) for $\{\eta^3\text{-HB(3-Bu}^t\text{pz)}_3\}\text{Zn(CN)}_{0.9}\text{I}_{0.1}$

atom	*x*	*y*	*z*	*U*[a]
Zn	1622 (1)	7500	5949 (1)	38 (1)
C	481 (7)	7500	5417 (15)	62 (4)
I	187 (5)	7500	5144 (11)	80 (4)
N	−210 (5)	7500	5063 (11)	93 (4)
N(11)	3288 (2)	7500	5141 (4)	42 (1)
N(12)	2533 (2)	7500	4522 (4)	42 (1)
N(21)	2952 (2)	8291 (2)	7297 (3)	41 (1)
N(22)	2134 (2)	8443 (2)	7104 (3)	38 (1)
C(11)	3876 (3)	7500	4197 (6)	50 (2)
C(12)	3513 (4)	7500	2920 (6)	57 (2)
C(13)	2677 (4)	7500	3153 (5)	48 (2)
C(14)	1974 (4)	7500	2120 (5)	59 (2)
C(15)	2333 (5)	7500	677 (5)	88 (3)
C(16)	1451 (3)	8294 (3)	2325 (4)	79 (2)
C(21)	3267 (2)	8893 (3)	8087 (4)	53 (1)
C(22)	2664 (2)	9453 (3)	8422 (4)	57 (1)
C(23)	1958 (2)	9157 (2)	7789 (3)	42 (1)
C(24)	1105 (2)	9524 (2)	7848 (4)	51 (1)
C(25)	1093 (3)	10270 (3)	8843 (6)	91 (2)
C(26)	497 (2)	8869 (3)	8400 (4)	58 (1)
C(27)	841 (3)	9813 (3)	6441 (5)	95 (2)
B	3380 (4)	7500	6710 (6)	43 (2)

[a] Equivalent isotropic *U* defined as one-third of the trace of the orthogonalized U_{ij} tensor.

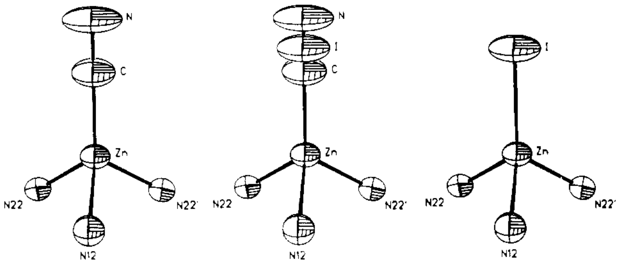

Figure 6. Partial ORTEP drawings for $(\text{CN})_{0.9}\text{I}_{0.1}$ (50% thermal ellipsoids) with disordered site refined as $(\text{CN})_{0.906(4)}\text{I}_{0.094(4)}$. Center: superposition of CN and I groups at the disordered site. Left and right: disordered site separated into composite molecules.

satisfactorily in the absence of a disorder model. Furthermore, the two distinct atom sites for C and Br was not resolved for this sample either, and an apparent C≡N bond length of 0.764 (24) Å was observed.

Although the disorder between (i) CN and Cl and (ii) CN and Br was not resolved, we have observed that disorder between cyanide and iodide in a crystal of composition $\{\eta^3\text{-HB(3-Bu}^t\text{pz)}_3\}\text{Zn(CN)}_{0.9}\text{I}_{0.1}$ is readily resolved, in that three peaks are observed in the electron density difference map. The partial ORTEP drawing shown in Figure 6 illustrates the solution that is obtained by refining the cyanide and iodide groups with partial occupancies. The composition of the crystal as determined by this refinement procedure is $\{\eta^3\text{-HB(3-Bu}^t\text{pz)}_3\}\text{Zn(CN)}_{0.906(4)}\text{I}_{0.094(4)}$, in very close agreement with that determined by ^{1}H NMR spectroscopy. Figure 6 also illustrates the partial ORTEP drawings for the resolved structures, and comparison with the ORTEP drawings of the pure complexes suggests that the refinement procedure used is successful. Atomic coordinates are presented in Table V. However, how well do the bond lengths of the resolved structures compare with those of the true structures of the pure complexes $\{\eta^3\text{-HB(3-Bu}^t\text{pz)}_3\}\text{ZnCN}$ and $\{\eta^3\text{-HB(3-Bu}^t\text{pz)}_3\}\text{ZnI}$? Table II lists selected bond lengths for $\{\eta^3\text{-HB(3-Bu}^t\text{pz)}_3\}\text{Zn(CN)}_{0.9}\text{I}_{0.1}$, $\{\eta^3\text{-HB(3-Bu}^t\text{pz)}_3\}\text{ZnCN}$, and $\{\eta^3\text{-HB(3-Bu}^t\text{pz)}_3\}\text{ZnI}$. It is evident from Table II that the Zn–CN and Zn–I moieties of the resolved structures compare reasonably well with those of the pure compounds, and thus the disordered model is useful. However, the observed bond lengths are *not* identical with the true values. For example, the Zn–I bond length of 2.469(8) Å for the disordered structure is slightly shorter than that observed for pure $\{\eta^3\text{-HB(3-Bu}^t\text{pz)}_3\}\text{ZnI}$ [2.518(1) Å],[6] the C–N bond length of 1.178 (15) Å is longer than that in $\{\eta^3\text{-HB(3-Bu}^t\text{pz)}_3\}\text{ZnCN}$ [1.117 (9) Å], and the Zn–C bond length of 1.932 (12) Å is slightly shorter than that in $\{\eta^3\text{-HB(3-Bu}^t\text{pz)}_3\}\text{ZnCN}$ [1.962 (6) Å]. Indeed, it is interesting that these small differences are not all in the direction that may be expected due to the disorder. In particular, a slight apparent shortening of the Zn–C bond is unexpected and may represent an artifact of the treatment. Therefore, although resolved structures obtained by such a refinement procedure may be taken as good evidence for the nature of the disorder, bond lengths derived from disordered structures should be treated with caution, especially when accurate structural details are required.

The above results demonstrate that disorder between CN and I was resolved, even though the disorder between (i) CN and Cl and (ii) CN and Br was not. The reason behind these differences is undoubtedly a consequence of the relative positions of the disordered groups. For CN/I, the I atom is located approximately midway between C and N, 0.56 Å from C. However, for CN/Cl and CN/Br, the halogen atoms are located much closer to C, at distances of 0.22 and 0.36 Å, respectively. Although early work suggested that the limit of resolution for an X-ray diffraction experiment is $0.61d_{\min}$ (where $d_{\min} = \lambda/(2 \sin \theta)$),[22] Stenkamp

Table VI. Selection of Structures in Which Disorder between Diatomic and Monatomic Groups Occurs

disordered system	*d*(M–X)/Å	*d*(M–YZ)/Å	*d*(X···Y)/Å	$d_{\min}$/Å	*d*(X···Y)/$d_{\min}$	resolved	ref
$\{\eta^3\text{-HB(3-Bu}^t\text{pz)}_3\}\text{Zn(CN)}_x\text{Cl}_{1-x}$	2.183 (2)[a]	1.962 (6)[a]	0.22	0.77	0.29	no	*f*
$\{\eta^3\text{-HB(3-Bu}^t\text{pz)}_3\}\text{Zn(CN)}_x\text{Br}_{1-x}$	2.325 (1)[a]	1.962 (6)[a]	0.36	0.77	0.47	no	*f*
$\{\eta^3\text{-HB(3-Bu}^t\text{pz)}_3\}\text{Zn(CN)}_x\text{I}_{1-x}$	2.518 (1)[a]	1.962 (6)[a]	0.56	0.77	0.73	yes	*f*
$[\text{Mo(PMe}_3)_4(\text{N}_2)_2]/[\text{Mo(PMe}_3)_4\text{Cl}_2]$	2.420 (6)[a]	2.08 (1)[b]	0.34	0.84	0.40	yes	*g*
$[\text{W(PMe}_3)_4(\text{N}_2)_2]/[\text{W(PMe}_3)_4\text{Cl}_2]$	2.46 (1)[b]	2.04 (2)[b]	0.42	0.84	0.50	yes	*g*
$[\text{Cr(dmpe)}_2(\text{N}_2)_2]/[\text{Cr(dmpe)}_2\text{Cl}_2]$	2.35 (1)[c]	1.874 (3)[b]	0.48	0.84	0.57	no	*h*
$\text{ReCl(N}_2)(\text{PMe}_2\text{Ph})_4$	2.521 (4)[b]	1.97 (2)[b]	0.55	1.18	0.47	no	*i*
trans-$\text{IrCl(CO)(PPh}_3)_2$	2.382 (3)[b]	1.791 (13)[b]	0.59	0.84	0.70	yes	*j*
trans-$\text{RhCl(CO)(PPh}_3)_2$	2.395 (1)[d]	1.821 (5)[d]	0.57	0.84	0.68	no	*k*
trans-$\text{IrCl(CO)[P(}o\text{-MeC}_6\text{H}_4)_3]_2$	2.43 (1)[b]	1.67 (4)[b]	0.76	1.04	0.73	yes	*l*
trans-$\text{IrCl(CO)[P(}p\text{-MeC}_6\text{H}_4)_3]_2$	2.364 (2)[b]	1.817 (8)[b]	0.55	0.93	0.59	yes	*m*
trans-$\text{Ir(CH}_3)(\text{CO)(PPh}_3)_2$	2.17[e]	1.84[e]	0.33	0.84	0.39	no	*n*

[a] Bond lengths obtained independently for a pure crystal. [b] Bond lengths obtained from the disordered structure. [c] Average Cr–Cl bond length in $\text{Cr(dmpe)}_2\text{Cl}_2$ [2.351 (3) and 2.345 (3) Å] (see third reference in footnote *h*). [d] Bond lengths for an *ordered* polymorph (see first reference in footnote *k*). [e] Estimated values determined from a disordered structure. [f] This work. [g] Carmona, E.; Martin, J. M.; Poveda, M. L.; Atwood, J. L.; Rogers, R. D. *Polyhedron* **1983**, *2*, 185–193. [h] Girolami, G. S.; Salt, J. E.; Wilkinson, G.; Thornton-Pett, M.; Hursthouse, M. B. *J. Am. Chem. Soc.* **1983**, *105*, 5954–5956. Salt, J. E.; Girolami, G. S.; Wilkinson, G.; Motevalli, M.; Thornton-Pett, M.; Hursthouse, M. B. *J. Chem. Soc., Dalton Trans.* **1985**, 685–692. Girolami, G. S.; Wilkinson, G.; Galas, A. M. R.; Thornton-Pett, M.; Hursthouse, M. B. *J. Chem. Soc., Dalton Trans.* **1985**, 1339–1348. [i] Davis, B. R.; Ibers, J. A. *Inorg. Chem.* **1971**, *10*, 578–585. [j] Churchill, M. R.; Fettinger, J. C.; Buttrey, L. A.; Barkan, M. D.; Thompson, J. S. *J. Organomet. Chem.* **1988**, *340*, 257–266. [k] Rheingold, A. L.; Geib, S. J. *Acta Crystallogr.* **1987**, *C43*, 785–786. Del Pra, A.; Zanotti, G.; Segula, P. *Cryst. Struct. Commun.* **1979**, *8*, 959–964. [l] Brady, R.; De Camp, W. H.; Flynn, B. R.; Schneider, M. L.; Scott, J. D.; Vaska, L.; Werneke, M. F. *Inorg. Chem.* **1975**, *14*, 2669–2675. [m] Churchill, M. R.; Fettinger, J. C.; Rappoli, B. J.; Atwood, J. D. *Acta Crystallogr.* **1987**, *C43*, 1697–1699. [n] Rees, W. M.; Churchill, M. R.; Li, Y-J.; Atwood, J. D. *Organometallics* **1985**, *4*, 1162–1167.

Table VII. Summary of Crystal and Intensity Collection Data

	LZnCN	LZn(CN)$_{0.8}$Cl$_{0.2}$	LZn(CN)$_{0.95}$Br$_{0.05}$	LZn(CN)$_{0.9}$I$_{0.1}$
formula	$C_{22}H_{34}N_7BZn$	$C_{21.8}H_{34}N_{6.8}BZnCl_{0.2}$	$C_{21.95}H_{34}N_{6.95}BZnBr_{0.05}$	$C_{21.9}H_{34}N_{6.9}BZnI_{0.1}$
lattice	orthorhombic	orthorhombic	orthorhombic	orthorhombic
a/Å	16.315 (3)	16.235 (2)	16.303 (4)	16.315 (6)
b/Å	15.852 (3)	15.871 (3)	15.847 (6)	15.841 (8)
c/Å	9.757 (2)	9.760 (1)	9.752 (3)	9.751 (4)
V/Å^2	2523 (1)	2514 (1)	2519 (1)	2520 (1)
Z	4	4	4	4
space group	*Pnma* (No. 62)	*Pnma* (No. 62)	*Pnma* (No. 62)	*Pnma* (No. 62)
radiation (λ, Å)	Mo Kα (0.71073)	Mo Kα (0.71073)	Mo Kα (0.71073)	Mo Kα (0.71073)
μ(Mo Kα), cm^{-1}	10.3	10.5	11.1	11.5
ρ(calcd), g cm^{-3}	1.25	1.25	1.25	1.27
temp	room temp	room temp	room temp	room temp
goodness of fit	1.240	1.104	1.495	1.278
R^a	0.0397	0.0374	0.0428	0.0404
$R_w{}^a$	0.0421	0.0479	0.0625	0.0458

$^a R = \sum||F_o| - |F_c||/\sum|F_o|$; $R_w = \{[\sum(F_o - F_c)^2]/[\sum w(F_o)^2]\}^{1/2}$; GOF $= \{[\sum w(F_o - F_c)^2]/[N_{data} - N_{params}]\}^{1/2}$; $w - [\sigma^2(F) + gF^2]^{-1}$.

and Jensen have more recently proposed that the limit of resolution for point atoms in three-dimensional electron density maps is in fact $0.917d_{min}$.[23] Table VI compiles a list of some disordered structures, together with the distances between the disordered atoms, and also the values of d_{min} for the data collection. Examination of the ratios $d(X\cdots Y)/d_{min}$ reveals that it is not unanticipated that disorder between CN/Cl and CN/Br, with atom separations of $0.29d_{min}$ and $0.47d_{min}$, respectively, was not resolved. However, the disordered atoms for the CN/I system are separated by only $0.73d_{min}$, and yet may be readily resolved.[24] Indeed, further inspection of Table VI indicates that resolution of a disordered site has been achieved for atoms that are separated by as little as $0.40d_{min}$. It is possible that resolution which is apparently better than $0.917d_{min}$ may be an artifact of the peak-searching routine, which need not necessarily locate a true electron density maximum.

Conclusion

The above studies have provided more evidence for the occurrence of disorder of structurally inequivalent groups at a single crystallographic site. By use of a technique in which a crystal is doped with an impurity, the disorder at a single site was varied in a controlled fashion. In this manner we have demonstrated that whereas the disorder between CN and I was readily resolved, the disorder between (i) CN and Cl and (ii) CN and Br was not resolved. For the {η^3-HB(3-Bu^{t}pz)$_3$}Zn(CN)$_x$Br$_{1-x}$ disordered system, the apparent C–N bond length was a function of the composition, varying from 1.058 (9) Å for $x = 0.95$ to 0.764 (24) Å for $x = 0.55$. Although the anomalous thermal parameters of the C and N atoms for the crystal of composition {η^3-HB(3-Bu^{t}pz)$_3$}Zn(CN)$_{0.55}$Br$_{0.45}$ revealed a disordered site, a crystal of composition {η^3-HB(3-Bu^{t}pz)$_3$}Zn(CN)$_{0.95}$Br$_{0.05}$ refined well as {η^3-HB(3-Bu^{t}pz)$_3$}ZnCN, with no obvious indication of an anomaly, even though the C–N bond length was incorrect. The disorder between CN and I in {η^3-HB(3-Bu^{t}pz)$_3$}Zn(CN)$_{0.9}$I$_{0.1}$ was readily apparent, and the individual groups could be refined with surprising success. However, despite this apparent success, the bond lengths obtained from the disordered structure were also incorrect, as judged by comparison with data for the pure structures. Thus, although satisfactory refinement of a disordered structure may be taken as good evidence for the nature of the disorder, and therefore a good indication of the molecular structure, attempts to extract the *true* bond lengths from such a structure must be treated with caution: although the observed bond lengths obtained by such a procedure *may* be correct, they are not necessarily so. Indeed, consideration of this issue is particularly relevant in evaluating structures for which accurate structural parameters are required, such as in proposed examples of bond-stretch isomerism.

Experimental Section

All manipulations were performed using a combination of glovebox, high-vacuum, or Schlenk techniques.[25] Solvents were purified and degassed by standard procedures. NMR spectra were recorded on Varian VXR 300 and 400 spectrometers. Crystals of pure {η^3-HB(3-Bu^{t}pz)$_3$}ZnCN and {η^3-HB(3-Bu^{t}pz)$_3$}Zn(CN)$_x$X$_{1-x}$ (X = Cl, Br, I) mixtures were obtained from concentrated dichloromethane or THF solutions at room temperature. After X-ray data collection, the composition of each crystal was determined by ^{1}H NMR spectroscopy. In most cases, similar compositions were also measured for the bulk sample.

Preparation of {η^3-HB(3-Bu^{t}pz)$_3$}ZnX (X = CN, Cl, Br, I). The complexes {η^3-HB(3-Bu^{t}pz)$_3$}ZnX were prepared by reaction of {HB(3-Bu^{t}pz)$_3$}K with ZnX$_2$, and a typical procedure, similar to that reported previously,[26] is given below. A solution of {HB(3-Bu^{t}pz)$_3$}K (2.0 g, 4.76 mmol) in THF (40 mL) was added to a stirred suspension of Zn(CN)$_2$ (1.12 g, 9.52 mmol) in THF (40 mL), depositing a white precipitate. The mixture was stirred overnight at room temperature and filtered. The solvent was removed from the colorless filtrate under reduced pressure, giving {η^3-HB(3-Bu^{t}pz)$_3$}ZnCN as a white solid (1.87 g, 83%). ^{1}H NMR data (C_6D_6): δ 1.47 [s, $C_3N_2H_2C(CH_3)_3$], 5.75 and 7.21 [d, $^3J_{H-H} = 2.2$ Hz, $C_3N_2H_2C(CH_3)_3$].

X-ray Structure Determination Procedures. Crystal data and data collection and refinement parameters for the structures reported are summarized in Table VII. Complete tables of crystal data and data collection and refinement parameters are given in the supplementary material. A typical procedure for the structure determination is as follows. A single crystal was mounted in a glass capillary and placed on a Nicolet R3m diffractometer. The unit cell was determined by the automatic indexing of 25 centered reflections and confirmed by examination of the axial photographs. Intensity data were collected using graphite-monochromated Mo Kα X-radiation (λ = 0.71073 Å) at room temperature. Check reflections were measured every 100 reflections, and the data were scaled accordingly and corrected for Lorentz, polarization, and absorption effects. The structure was solved by direct methods and standard difference map techniques on a Data General NOVA 4 computer using SHELXTL.[27] Systematic absences were consistent with the space groups *Pnma* and *Pna*2$_1$, but consideration of the *E* value statistics suggested the choice *Pnma* (No. 62). Hydrogens on carbon were included in calculated positions ($d_{C-H} = 0.96$ Å; $U_{iso}(H) = 1.2U_{iso}(C)$). For the chloride, bromide, and iodide solid solutions, the disordered site was modeled by refining the site occupancies subject to the constraints (i) that carbon and nitrogen maintain a common value and (ii) that the sum of the carbon and halide site occupancies be 0.5 (the disordered site lies on a mirror plane). The compositions determined by this refinement pro-

---

(22) James, R. W. *The Optical Principles of the Diffraction of X-rays.* Ox Bow Press: Woodbridge, CT, 1982.

(23) Stenkamp, R. E.; Jensen, L. H. *Acta Crystallogr.* **1984**, *A40*, 251–254.

(24) The suceesssful resolution of CN and I is also particularly interesting, given our inability to resolve the disorder for the related CH$_3$/I system, i.e. {η^3-HB(3-Bu^{t}pz)$_3$}Zn(CH$_3$)$_x$I$_{1-x}$, for which the separation between C and I is 0.55 Å. See ref 6.

(25) (a) McNally, J. P.; Leong, V. S.; Cooper, N. J. *ACS Symp. Ser.* **1987**, *357*, 6–23. (b) Burger, B. J.; Bercaw, J. E. *ACS Symp. Ser.* **1987**, *357*, 79–97.

(26) Trofimenko, S.; Calabrese, J. C.; Thompson, J. S. *Inorg. Chem.* **1987**, *26*, 1507–1514.

(27) Sheldrick, G. M. SHELXTL: An integrated System for Solving, Refining and Displaying Crystal Structures from Diffraction Data. University of Göttingen, Göttingen, Germany, 1981.

cedure compared well with those determined by ^{1}H NMR analysis.[28] Complete tables of atomic coordinates, bond distances and angles, and anisotropic displacement parameters and ORTEP drawings for all structures are given in the supplementary material.

Acknowledgment. This work was supported by the National Science Foundation (Grant CHE-9007512). G.P. is the recipient of an A. P. Sloan Research Fellowship (1991–1993) and a Camille and Henry Dreyfus Teacher-Scholar Award (1991–1996). We thank Professor R. E. Marsh and the reviewers for very helpful comments.

Registry No. $\{\eta^3\text{-HB(3-Bu}^t\text{pz)}_3\}$ZnCN, 127623-01-2.

Supplementary Material Available: Tables SI–SXXX, giving crystal and intensity collection data, atomic coordinates, bond distances and angles, and anisotropic displacement parameters, and ORTEP drawings for all structures (35 pages); listings of calculated and observed structure factors (50 pages). Ordering information is given on any current masthead page.

---

(28) $\{\eta^3\text{-HB(3-Bu}^t\text{pz)}_3\}\text{Zn(CN)}_x\text{Cl}_{1-x}$: x(NMR) = 0.80, x(X-ray) = 0.76. $\{\eta^3\text{-HB(3-Bu}^t\text{pz)}_c\}\text{Zn(CN)}_x\text{Br}_{1-x}$: x(NMR) = 0.95, x(X-ray) = 0.96. $\{\eta^3\text{-HB(3-Bu}^t\text{pz)}_3\}\text{Zn(CN)}_x\text{Br}_{1-x}$: x(NMR) = 0.55, x(X-ray) = 0.56. $\{\eta^3\text{-HB(3-Bu}^t\text{pz)}_3\}\text{Zn(CN)}_x\text{I}_{1-x}$: x(NMR) = 0.90, x(X-ray) = 0.91.

Contribution from the Department of Chemistry and the UWM-NIEHS Aquatic and Marine Biomedical Core Center,
University of Wisconsin—Milwaukee, P.O. Box 413, Milwaukee, Wisconsin 53201

Biphasic Reactions of DTNB with Lobster Cd_6- and Cd_5Cu-Metallothionein-2 Which Have Two Type-B (M_3S_9) Clusters

Zhiwu Zhu, Mark Goodrich, Anvarhusein A. Isab,[†] and C. Frank Shaw III*

Received July 17, 1991

Lobster metallothionein (MT), which has two three-metal clusters instead of the four-metal and three-metal clusters found in mammalian MTs, was used to determine the origin of the biphasic reactions of MT with DTNB. Cd-rich MTs (Cd_5Cu-MT-2 and Cd_6-MT-2) were isolated from lobster hepatopancreas after Cd treatment preceded by dexamethasone injection or an applied stress. Each lobster MT-2 preparation reacts biphasically with DTNB [5,5′-dithiobis(2-nitrobenzoic acid)], as do mammalian MTs, and the reaction proceeds about 1 order of magnitude faster than that of mammalian MTs. The slow step and fast step each have first- and second-order components, resulting in a four-term rate law: rate = $k_{1s} + k_{2s}[\text{DTNB}] + k_{1f} + k_{2f}[\text{DTNB}]$. At 25 °C, in 5 mM Tris/HCl buffer with 100 mM KCl, at pH 7.4, the rate constants are $k_{1s} = 1.34 \times 10^{-3}$ s^{-1}, $k_{2s} = 0.706$ s^{-1} M^{-1}, $k_{1f} = 3.23 \times 10^{-3}$ s^{-1}, $k_{2f} = 2.92$ s^{-1} M^{-1} for Cd_5Cu-MT-2; $k_{1s} = 1.23 \times 10^{-3}$ s^{-1}, $k_{2s} = 0.663$ s^{-1} M^{-1}, $k_{1f} = 2.27 \times 10^{-3}$ s^{-1}, $k_{2f} = 8.13$ s^{-1} M^{-1} for Cd_6-MT-2. The biphasic nature of these reactions establish that the MT amino acid sequences, and not the structures of the individual clusters, determine the reactivity toward DTNB. Comparison of the lobster MT sequence with those for mammalian MTs leads to the prediction that the clusters of crustacean MTs are also located in separate domains. Consistent with this prediction, the presence of a single copper reduces the rate of the fast step, but does not alter the slow step for lobster MT-2.

Metallothionein (MT)[1] is a small protein which is rich in highly-conserved cysteine residues and able to bind various metal ions including Zn(II), Cd(II), Au(I), Ag(I), Cu(I), Hg(II), and Pt(II). Interest in MT has stimulated intensive research over the last several decades.[1-3] It is believed that MT plays an important role in metal ion metabolism.[4-8] A great deal of research has been done on the elucidation of the structure of this protein. Homonuclear ^{113}Cd decoupling studies[9] revealed the existence of two clusters, type A and type B, able to bind four and three metal ions, respectively. These ions are tetrahedrally coordinated by terminal and bridging thiolates from the cysteine residues of the protein. Further studies revealed that each cluster was in a separate domain of the protein (M_4S_{11} in the α-domain and M_3S_9 in the β-domain).[10] Subsequent 2-D NMR and X-ray studies confirmed this conclusion.[11-13] However, much less has been done to characterize the reactivity and putative functions of MT in terms of its unique structure. In order to fully characterize this protein, the linkage between structure and reactivity must be determined.

Examining the kinetics of bioinorganic reactions between MT and various ligands[1,14] and electrophiles[15-18] has enlarged our understanding of the reactivity of MT. The well-studied reactions of mammalian MTs with DTNB,[15,17] which attacks the metal-bound thiolates, show biphasic kinetics. Possible origins might include differential reactivity of the two domains or different rates for terminal and bridging thiolates. Any differences in reactivity of the domains might be intrinsic to the two metal–thiolate clusters or imposed by the protein chain. Kinetic studies of the reaction of rabbit liver MT α-cluster domain[17] narrowed the number of possibilities by eliminating the differences in the reactivity of bridging and terminal thiolates' MT as a possible cause. Whether the two clusters themselves or the sequences surrounding them cause the biphasic kinetics remain unanswered.

MTs from marine crustaceans[6,7,19-22] will provide important

---

[†] Department of Chemistry, King Fahd University of Petroleum and Minerals, Dhahran, 31261, Saudi Arabia.

(1) Kagi, J. H. R.; Kojima, Y. *Metallothionein II*; Birkhauser Verlag: Basel, 1987.
(2) Otvos, J. D.; Petering, D. H.; Shaw, C. F., III. *Comments Inorg. Chem.* **1989**, *9*, 1–35.
(3) Hamer, D. H. *Ann. Rev. Biochem.* **1986**, *55*, 913–952.
(4) Petering, D. H.; Fowler, B. A. *Environ. Health Perspect.* **1986**, *65*, 217–224.
(5) Engel, D. W. *Biol. Bull.* **1987**, *172*, 69–82.
(6) Brouwer, M.; Brouwer, T. M.; Engel, D. W. *Mar. Environ. Res.* **1984**, *14*, 71–88.
(7) Engel, D. W.; Brouwer, M. *Mar. Environ. Res.* **1984**, *13*, 177–194.
(8) Karin, M. *Cell* **1985**, *41*, 9–10.
(9) Otvos, J. D.; Armitage, I. M. *Proc. Natl. Acad. Sci. U.S.A.* **1980**, *77*, 7094–7098.
(10) Winge, D. R.; Miklossy, K.-A. *J. Biol. Chem.* **1982**, *257*, 3471–3476.
(11) Robbins, A. H.; McRee, D. E.; Williamson, M.; Collett, S. A.; Xuong, N. H.; Furey, W. F.; Wang, B. C.; Stout, C. D. *J. Mol. Biol.* **1991**.
(12) Frey, M. H.; Wagner, G.; Vasak, M.; Sorensen, O. W.; Neuhaus, D.; Worgotter, E.; Kagi, J. H. R.; Ernst, R. R.; Wutrich, K. *J. Am. Chem. Soc.* **1985**, *107*, 6847–6851.
(13) Arseniev, A.; Schultze, P.; Worgotter, E.; Braun, W.; Wagner, G.; Vasak, M.; Kagi, J. H. R.; Wutrich, K. *J. Mol. Biol.* **1988**, *201*, 637–657.
(14) Li, Ti.-Y.; Kraker, A. J.; Shaw, C. F., III; Petering, D. H. *Proc. Natl. Acad. Sci. U.S.A.* **1980**, 77, 6334–6338.
(15) Li, Ti.-Y.; Minkel, D. T.; Shaw, C. F., III; Petering, D. H. *Biochem. J.* **1981**, *193*, 441–446.
(16) Shaw, C. F., III; Laib, J. E.; Savas, M. M.; Petering, D. H. *Inorg. Chem.* **1990**, *29*, 403–408.
(17) Savas, M. M.; Petering, D. H.; Shaw, C. F., III. *Inorg. Chem.* **1991**, *30*, 581–583.
(18) Bernhard, W. R.; Vasak, M.; Kagi, J. H. R. *Biochemistry* **1986**, *25*, 1975–1980.
(19) Viarengo, A. *CRC Critical Reviews in Aquatic Sciences*; CRC Press: Boca Raton, FL, 1989; Vol. 1, pp 295–317.